Journal of Molecular Structure 1199 (2020) 127004

Contents lists available at ScienceDirect

Journal of Molecular Structure

journal homepage: http://www.elsevier.com/locate/molstruc

Synthesis and DFT studies of the structure - NLO activity evaluation of 2-(4-methoxyphenyl)-1,4,5-triphenyl-2,5-dihydro-1*H*-imidazole

Rajeev.T. Ulahannan [a], V. Kannan [b, *], V. Vidya [b], K. Sreekumar [c]

[a] Department of Physics, Pavanatma College Murickassery, Idukki District, Kerala, 685604, India
[b] Department of Chemistry, Government College Kattappana, Idukki District, Kerala, 685508, India
[c] Department of Applied Chemistry, Cochin University of Science and Technology, Kochi, 22, Kerala, India

ARTICLE INFO

Article history:
Received 16 May 2019
Received in revised form
28 August 2019
Accepted 29 August 2019
Available online xxx

Keywords:
DFT calculations
Fukui function
Tetra-substituted imidazoles
X-ray sturcture

ABSTRACT

Synthesis, characterisation and single crystal X-Ray studies of 2-(4-methoxyphenyl)-1,4,5-triphenyl-2,5-dihydro-1H-imidazole are reported. Here after the compound is denoted as TSI. Small Angle X-Ray Diffraction (SXRD) showed that the crystal belonged to Monoclinic, $P2_1/c$ group. The electronic and structural properties of TSI were investigated by DFT and TD-DFT methods. This molecule is a good candidate to be used in OLED devices because of high electron transport mobility and low λ_e value. The difference between λ_e and λ_h is smaller so that it has a better hole-electron transport balance in OLED devices. The calculated static first order hyperpolarizability β(000), showed that the material exhibited good non-linear optical behaviour and could be used for NLO devices. Fukui indices were calculated to identify the reactive sites of the title compound.

1. Introduction

Imidazoles are important raw materials for fine chemical synthesis. They possess remarkable biological activity [1]. They have been used in applications such as anticancer [2], antibacterial [3], antiviral [4] antihypertensive [5] agents and antagonistic histamine receptors [6]. Certain imidazole derivatives are characterised by good electroluminescence properties (EL) [7–13] with excellent electron transport ability [14–16]. Substituted phenanthroimidazoles were recently reported as flurophores in non doped blue organic light emitting diodes [17,18]. A combined experimental and theoretical study on phenanthroimidazole-styryltriphenylamine derivatives has been reported by Thanikachalam et al. [19]. Imidazole derivatives were also used in solution processed organic-light emitting diode applications [20]. Some imidazole derivatives were used as efficient red phosphorescent OLEDs [21]. Demand for a suitable and better OLED material is still growing; imidazole moiety having electron donating and electron withdrawing groups will show better efficiency. A detailed investigation of the spectral properties, crystal structure and other theoretical analysis could give important information regarding structure, reactivity and applications in optoelectronics and drug designing.

The electronic and spectral properties of the title compound were studied using density functional theory (DFT) at the ground state and time dependent density functional theory (TD-DFT) at the excited state. The optimized geometry of the molecule, absorption spectra, electronic properties and nonlinear optical properties were studied with a view to get vital information regarding synthesis and design of new optical devices. The choice of a material to be used in OLED devices is dependent on its low ionisation energy, low reorganisation energy, high electron affinity and high electron carrier mobility. Studies on these features are reported in this work.

2. Experimental details

Commercial clay used in this work was montmorillonite K10 which was purchased from Sigma-Aldrich, India and modified by ion exchange of Ti^{4+} by wet chemical method. The modified clay was activated at 200 °C for 3 h prior to use. All other reagents were purchased from Merck Ltd. India and were used as such. The product obtained was characterised by, ^{1}HNMR, FT-IR spectral methods, SXRD and m.p. FT-IR spectrum was recorded by the KBr pellet method on a JASCO FT-IR spectrometer in the range of 400–4000 cm^{-1}.^{1}H NMR spectrum was recorded on a Bruker 400 MHz instrument with tetramethyl silane (TMS) as internal

* Corresponding author.
E-mail address: kannanpvl@gmail.com (V. Kannan).

https://doi.org/10.1016/j.molstruc.2019.127004
0022-2860/

standard in $CDCl_3$.

2.1. Computational details

Computational study of the compound, 2-(4-methoxyphenyl)-1,4,5-triphenyl-2,5-dihydro-1*H*-imidazole was carried out with Gaussian 09 [22] program in the ground state using the B3LYP/6-31G basis set to obtain the optimized molecular structure and frequencies corresponding to its vibrational modes. Optimization of molecular structure was done by Berny's optimization algorithm using redundant internal coordinates [23]. A scaling factor of 0.9613 was used for obtaining a considerably better agreement with experimental data; because, the DFT hybrid B3LYP method might tend to overestimate the fundamental modes. The structure deduced was confirmed to be of minimum energy because of the absence of imaginary wave numbers on the calculated vibrational spectrum. The animation option of GAUSSVIEW program gave a visual presentation of the vibrational modes [24]. The absorption and emission of the molecule were studied from the TD-DFT studies on the molecule as this method was a very successful one to compute the excited states [25,26]. The energy of neutral molecule optimized in neutral state, energy of neutral molecule optimized in cation state, energy of cation state optimized in neutral state and energy of neutral molecule optimized in anion state were obtained using the TD-DFT/B3LYP6-31G computations [27].

2.2. Synthesis of 2-(4-methoxyphenyl)-1,4,5-triphenyl-2,5-dihydro-1H-imidazole

The title compound was synthesised by solvent free synthesis by taking benzil (1 mmol), 4-methoxybezaldehyde (1 mmol), aniline (1 mmol), NH_4OAc (1.3 mol %) and 0.2 g activated K10 clay catalyst. The mixture was stirred at 120 °C [28]. The formation of the product was monitored by thin layer chromatography. After the completion of the reaction, hot ethanol was added to the mixture and the insoluble catalyst was filtered off. The pure product was obtained by column chromatography using hexane and ethyl acetate (8:2 v/v) as eluent. The purified product was recrystallised from ethanol. (Scheme 1).

2.3. X-ray diffraction studies

Single crystal X-ray diffraction patterns of *2-(4-methoxyphenyl)-1,4,5-triphenyl-2,5-dihydro-1H-imidazole* were collected on Bruker AXS Kappa Apex 2 CCD diffractometer. Data collection was carried out using APEX 2 (Bruker, 2004), Cell refinement was done with APEX 2/SAINT (Bruker, 2004) and data reduction with SAINT/XPREP (Bruker 2004). Structure was solved with SIR 92 program. Structure was refined with SHELXL 97, Molecular graphics was plotted with ORTEP-3 and Mercury.

3. Results and discussion

3.1. Molecular structure

The title compound was synthesised and characterised by ^1H NMR, FT-IR and SXRD. The results of SXRD showed that the crystal belonged to monoclinic system of space group $P2_1/c$. The crystal data obtained is summarised in Table .1. The bond parameters such as bond length and bond angle were calculated theoretically and experimental values obtained in SXRD analysis were compared. Good agreements between experimental and theoretical values were obtained. The results are shown in Table 2.

Experimental and optimized bond length and bond angles of the title compound were compared. A good agreement was observed and is given in Table 2. The root mean square deviation (RMSD) values of bond length and bond angles were calculated using the expression, $\mathrm{RMS} = \sqrt{\left(\frac{1}{n-1}\right)\sum_{i}^{n}(\nu_i^{calc} - \nu_i^{exp})^2}$. The RMSD for bond length was 0.459 Å and that for bond angle was 0.520°. Complete results of these studies are given in the supplementary data.

Hydrogen refinements were done by keeping aliphatic methyl CH_3 hydrogen fixed and refined by difference in electron density synthesis method and riding model is followed in phenyl ring.

Imidazoles are reported to show weak non covalent interaction. Indole-benzene reported to favours π-π stacking interaction [29].

Table 1
Crystal data and structure refinement for 2(4-methoxyphenyl)-1,4,5-triphenyl-2,5-dihydro-1*H*-imidazole.

Empirical formula	$C_{28}H_{22}N_2O$
Formula weight	$Mr = 402.47$
Temperature	$T = 296$ K
Wavelength	$\lambda = 0.71073$ Å
Volume	$V = 2165.9\ (4)$ Å^3
Space group	$P21/c$
Crystal system Dx,g cm^{-3}	Monoclinic, 1.234 Mgm^{-3}
Unit cell dimensions	$a = 10.5906\ (10)$ Å
	$b = 10.3985\ (8)$ Å
	$c = 20.193\ (2)$ Å
	$\alpha = 90°$
	$\beta = 103.105\ (4)°$
	$\gamma = 90°$
Z	4
$F(000)$	848.0
$F(000')$	848.38
hkl_{max}	14,13,26
Crystal size	0.25 × 0.25 × 0.20 mm
Reflections collected	3302 reflections with $I > 2\sigma(I)$
Independent reflections	5155 independent reflections [$R_{int} = 0.032$]
Refinement on F^2	H-atom parameters constrained
Least-squares matrix: full	H-atom parameters constrained
$R[F^2 > 2\sigma(F^2)] = 0.048$	$\Delta\rho max = 0.17$ e Å^{-3}
$wR(F^2) = 0.157$	$\Delta\rho min = -0.24$ e Å^{-3}
$S = 1.07$	
5155 reflections	
281 parameters	
0 restraints	

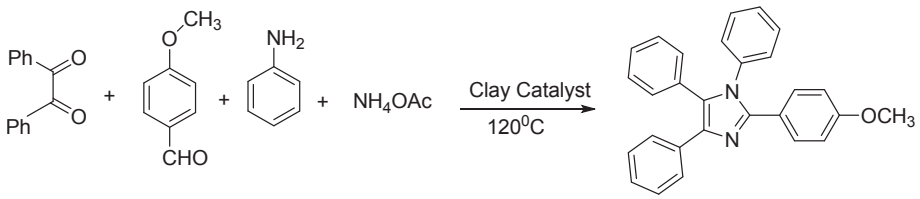

Scheme 1. Synthesis of 2(4-methoxyphenyl)-1,4,5-triphenyl-2,5-dihydro-1*H*-imidazole.

Table 2
The experimental and optimized bond length (Å) and bond angles for 2(4-methoxyphenyl)-1,4,5-triphenyl-2,5-dihydro-1*H*-imidazole.

Sl.No	Bond angle (θ)	Experimental	Optimized	Bond length(A^0)	Experimental	Optimized
1	$C_6C_1C_2$	121.15	120.29	C_2C_1	1.3751	1.3984
2	$C_2C_1N_2$	119.34	119.66	C_6C_1	1.3733	1.3981
3	$C_6C_1N_2$	119.44	120.05	N_2C_1	1.4349	1.4381
4	$H_2C_2C_1$	120.22	119.45	C_2H_2	0.9300	1.0807
5	$C_3C_2C_1$	119.57	119.74	C_3C_2	1.3764	1.3961
6	$H_2C_2C_3$	120.21	120.80	C_3H_3	0.9300	1.0814
7	$H_3C_3C_2$	119.85	119.66	C_3C_4	1.3555	1.3979
8	$C_4C_3C_2$	120.30	120.18	C_4H_4	0.9300	1.0815
9	$H_3C_3C_4$	119.85	120.15	C_4C_5	1.3727	1.3978
10	$H_4C_4C_3$	119.74	120.07	H_5C_5	0.9300	1.0814

X-Ray crystal studies showed a weak Van der Waals interaction between nearest molecules. Moreover imidazole-benzene favours π-π stacking interaction which helps the planar arrangement of each molecule in the unit cell. Each unit cell consists of four title molecule arranged in a regular fashion with almost all aromatic rings falling in the same plane leading to a packed structure.

3.2. ^{1}H NMR analysis of 2-(4-methoxyphenyl)-1,4,5-triphenyl-2,5-dihydro-1H-imidazole

The title compound 2(4-methoxyphenyl)-1,4,5-triphenyl-2,5-dihydro-1*H*-imidazolewas characterised by ^{1}HNMR recorded in $CDCl_3$(99.8 atom % D). The compound contains one set of aromatic protons in the region δ 6.75–7.60 and a set of aliphatic protons in the region δ 3.75. Signals of protons attached to C13, C17, C20, C24 are obtained as doublets around δ7.08–7.18. Singlet at δ 3.75 corresponds to the signal of isolated proton attached to C25. The results are shown in Fig. 2.

3.3. FT-IR analysis

Bands around 1486, 1440, 1367 and 1325 cm^{-1} are ascribed to C–N stretching frequencies of the imidazole ring [30,31]. Bands around 3100-3000 cm^{-1} indicate aromatic C–H stretching frequency of phenyl rings. C–C stretching vibrational bands are observed around 1400-1650 cm^{-1} [32]. C–C stretching vibrations of the title compound are observed around 1590 cm^{-1} in the FTIR spectrum. C–O–C stretching frequency of the title compound showed a medium band around 1275-1200 cm^{-1}. A characteristic band around 3000-3100 cm^{-1} indicates the presence of C–H stretching frequency in the molecule.

3.4. Reorganisation energy, HEP and EEP

The reorganisation energy (λ), ionisation energy (IE) and electron affinity (EA) were investigated to calculate the energy barrier for injection and transport rates of electrons and holes; as the charge transport/injection and its balance was decisive for opto-electronic materials. The ionisation energy (IE), electron affinity (EA) and reorganisation energy (λ) were obtained as follows;

$$I.E = E_0^+ - E_0^0$$

$$E.A = E_0^0 - E_0^-$$

The charge transfer rate K of electron or hole can be obtained from the Marcus/Hush model [33], as:

$$E.A = E_0^0 - E_0^-$$

where T is the temperature, k is the Boltzmann constant. The charge transfer rate is dependent on reorganisation energy and thus it is a very crucial factor in charge transfer proceses.

$$\lambda_e = \left(E_0^- - E_-^-\right) + \left(E_-^0 - E_0^0\right)$$

$$= \mathrm{EEP} - \mathrm{E.A}$$

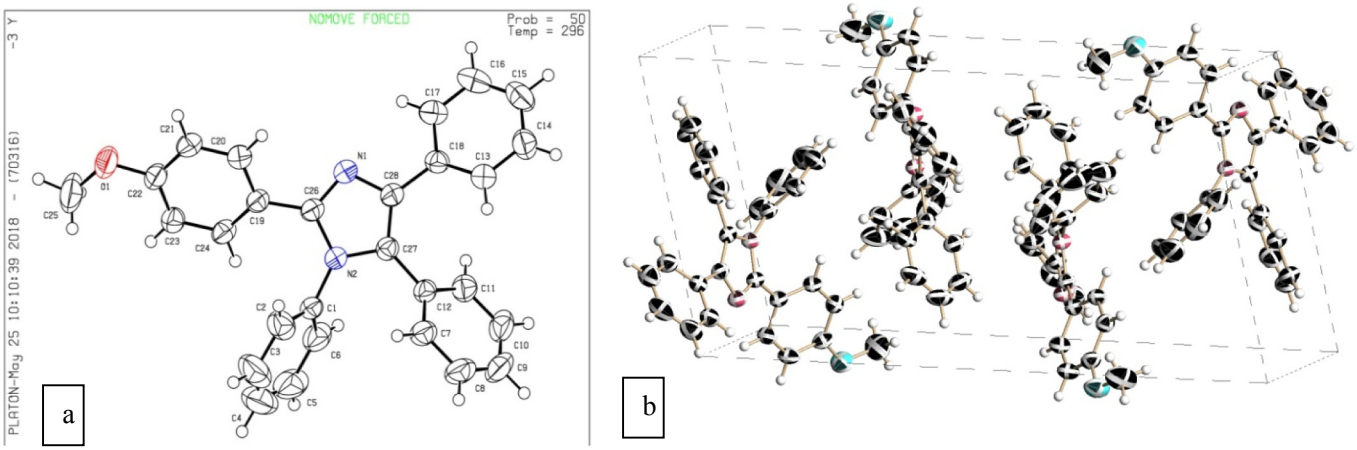

Fig. 1. a) Molecular structure of *2-(4-methoxyphenyl)-1,4,5-triphenyl-2,5-dihydro-1H-imidazole* showed the atom numbering scheme. Displacement ellipsoids are shown at the 50% probability level. **b)** Packing diagram of *2-(4-methoxyphenyl)-1,4,5-triphenyl-2,5-dihydro-1H-imidazole.*

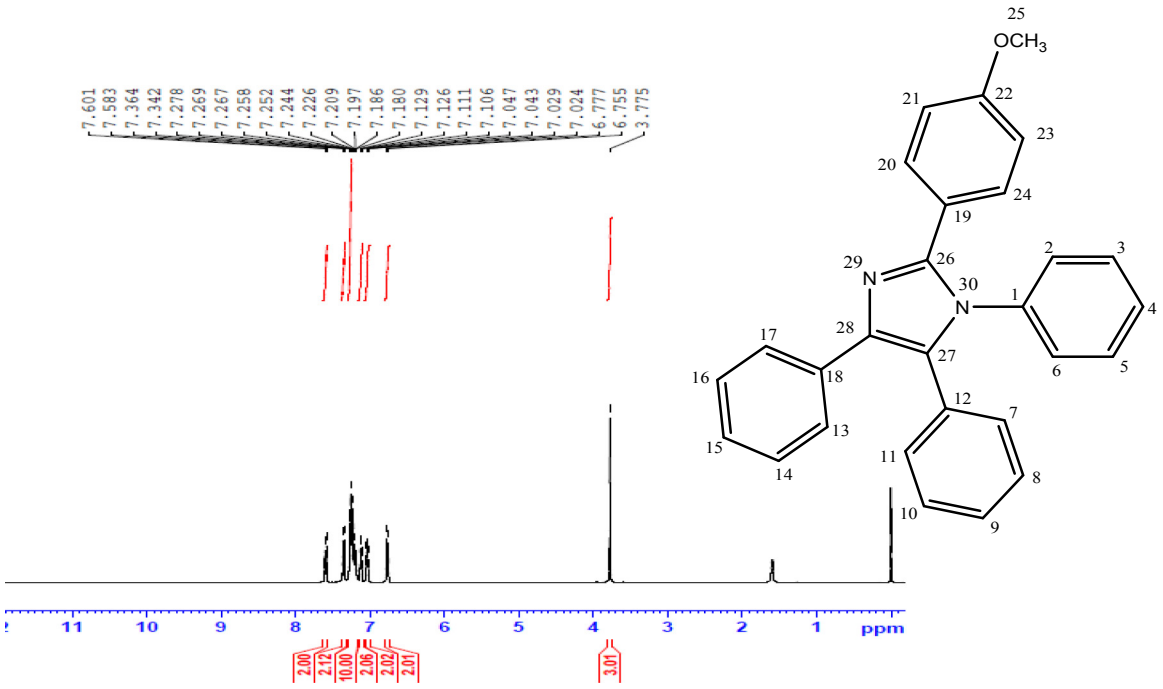

Fig. 2. ^{1}H NMR spectrum of 2-(4-methoxyphenyl)-1,4,5-triphenyl-2,5-dihydro-1*H*-imidazole.

$$\lambda_h = \left(E_0^+ - E_+^+\right) + \left(E_+^0 - E_0^0\right)$$

$$= \text{I.E} - \text{HEP}$$

Here λ_e is the reorganisation energy of electrons, λ_h that of holes. The electron extraction potential (EEP) is the difference in energy between the anion optimized in the neutral state and anion optimized in the anion state. The hole extraction potentials (HEP) is the energy difference between the cation optimized at cation state and anion optimized at anion state.

$$EEP = E_-^0 - E_-^-$$

$$HEP = E_+^+ - E_-^-$$

$E_0^0, E_0^-, E_0^+, E_+^0$ show the energy of neutral molecule optimized in neutral state, energy of neutral molecule optimized in anion state, energy of neutral molecule optimized in cation state, energy of cation state optimized in neutral state respectively. The calculated values of λ_e, λ_h, EEP, HEP, I.E and E.A are given in Table 3. The difference between λ_e and λ_h are very small suggesting that the present molecule has a better hole and electron transport balance. Such a material can act as an ambipolar material [34].

Table 3
Reorganisation energy.

HEP	6.235 eV
EEP	0.349 eV
λ_e	0.526 eV
λ_h	0.414 eV
I.E	6.649 eV
E.A	−0.176 eV

3.5. Frontier molecular orbital analysis

Imidazoles having optimum HOMO-LUMO separation have found wide applications in optoelectronic devices. The degree of intermolecular charge transfer between electron donor to electron acceptor group depends on the energy gap between HOMO and LUMO. It also determines the molecular stability and activity. Molecular orbital topology was calculated at DFT/6-31G levels. The frontier molecular orbitals were examined for characterising the electronic and optical properties. Molecular topologies of HOMO-LUMO orbitals of TSI are shown in Fig. 3. It is observed that HOMO is located mainly over imidazole ring and methoxy groups, whereas LUMO is located mainly on phenyl rings. The lowest unoccupied molecular orbital (LUMO) and highest occupied molecular orbital (HOMO) were visualised; E_{HOMO}, E_{LUMO} and energy gap (ΔE) were calculated.

Chemical reactivity can also be related to HOMO-LUMO energy gap, a molecule with small energy gap is more polarisable and highly reactive. The small HOMO-LUMO energy gap and a number of aromatic moiety suitable for π- π* transition indicates that the title compound is a good electron transport material.

3.6. Electronic properties

The absorption spectrum of the molecule was calculated using the TD-DFT method. The absorption wavelength, oscillator strength and corresponding absorption energies are listed in Table 4.

Experimental UV–Vis spectrum for *2-(4-methoxyphenyl)-1,4,5-triphenyl-2,5-dihydro-1H-imidazole* showed 2 absorption bands around 230 nm, 290 nm associated with π- π* transition of aromatic ring, which may be correlated to the bands calculated at 270.33 and 284.38 with oscillatory strength 0.0051 and 0.0119; these transitions are comparatively weak in solvents. The band around 330 nm is ascribed to π- π* transition within the C=N azomethine group [35]. This may be correlated to the band calculated at 325.29 nm having high oscillator strength 0.1249. The discrepancy between experimental and theoretical prediction

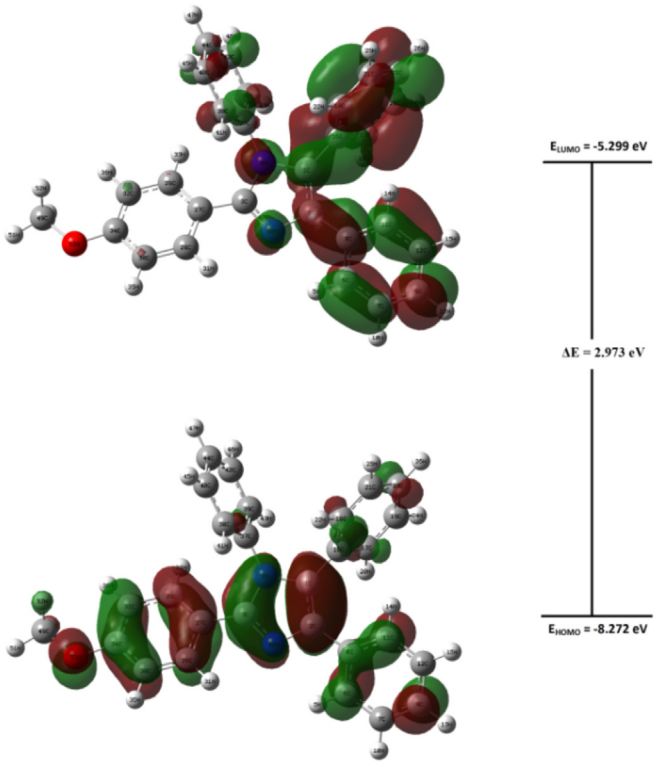

Fig. 3. HOMO-LUMO plot of 2(4-methoxyphenyl)-1,4,5-triphenyl-2,5-dihydro-1*H*-imidazole.

Table 4
Excitation energies and Oscillator strengths.

Excited states	Oscillator strength	E (eV)	λ(calculated)
106 ->107	f = 0.1249	3.8115 eV	325.29 nm
106 ->108			
106 ->109			
106 ->107	f = 0.0289	3.8973 eV	318.13 nm
106 ->108			
106 ->107	f = 0.1369	4.1129 eV	301.45 nm
106 ->109			
106 ->110			
105 ->107	f = 0.3623	4.3337 eV	286.09 nm
106 ->110			
106 ->111	f = 0.0119	4.3598 eV	284.38 nm
101 ->107	f = 0.0051	4.5864 eV	270.33 nm
101 ->110			
106 ->112			

could be the consequence of charge transfer valence-excited states that might occur in the molecule. The excited states 105, 106, 107, 108 represent HOMO-1, HOMO, LUMO and LUMO+1 respectively.

3.7. Molecular electrostatic potential (MEP)

The molecular electrostatic potential of a molecule gives information about the electrophilic and nucleophilic reactivity sites as well as hydrogen bonding interactions; it also offers a visual method for the understanding of polarity of the molecule [36]. The red represents the negative electrostatic potential region, blue represents the positive and green represents the zero potential regions; the other colours are intermediate such that, red ‹orange‹ yellow‹ green‹ blue gives the increasing order of electrostatic potential. Negative regions are associated with electron rich regions such as electronegative groups [37]. In the title compound, the regions of negative potential are concentrated over electronegative atoms (oxygen atom of methoxy group and nitrogen atoms of imidazole) Fig. 4.

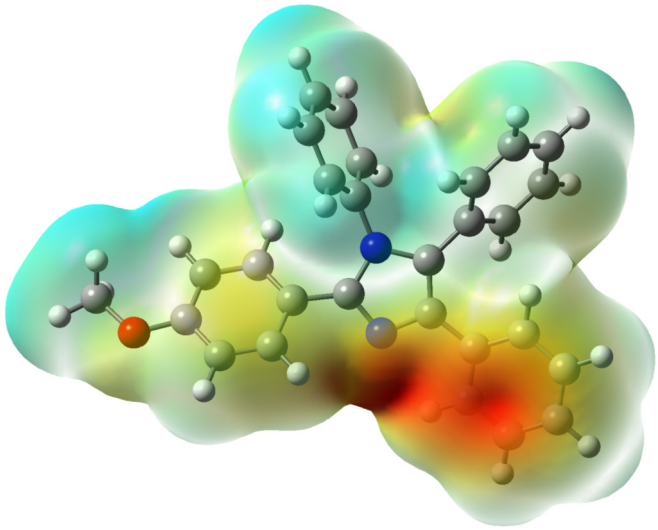

Fig. 4. MEP plot of 2(4-methoxyphenyl)-1,4,5-triphenyl-2,5-dihydro-1*H*-imidazole.

3.8. Fukui indices

Fukui indices determine the important reactive sites. Fukui indices indicate the tendency of the electronic density to deform at a given position by donating or accepting electrons [38,39]. Fukui functions on the jth atom site are defined as follows:

$$f_j^+ = q_j(N+1) - q_j(N)$$

$$f_j^- = q_j(N) - q_j(N-1)$$

$$f_j^0 = 0.5\left[q_j(N+1) - q_j(N-1)\right]$$

Fukui function for an electrophilic attack is denoted by f_j^+, nucleophilic or free radical attack f_j^- on the reference molecule, respectively. In these equations, q_j is the atomic charge (evaluated from Mulliken population analysis, electrostatic derived charge, etc.) at the jth atomic site in the neutral (N), anionic (N +1) or cationic (N - 1) chemical species. The concept of generalized electro (nucleo)- philicity has been introduced by Chattaraj et al. [40]. It contains information about different global and local reactivity descriptor and selectivity descriptor; the information regarding electrophilic/nucleophilic power of a given atomic site in a molecule. A dual descriptor$\Delta f(r)$, was proposed by Morell et al. [41], which was defined as the difference between the nucleophilic and electrophilic Fukui function and is given by,

$$\Delta f(r) = f^+(r) - f^-(r)$$

The site is favoured for a nucleophilic attack if $\Delta f(r) > 0$, the site may be favoured for an electrophilic attack if $\Delta f(r) < 0$. Thus dual descriptors $\Delta f(r)$ provide a clear difference between nucleophilic and electrophilic attack at a particular site with their sign. That is, they provide positive value for site prone for nucleophilic attack and a negative value to the site prone for electrophilic attack.

Fukui functions are evaluated from Mulliken population analysis and the results are given in graphical form in Fig. 5. The reactivity

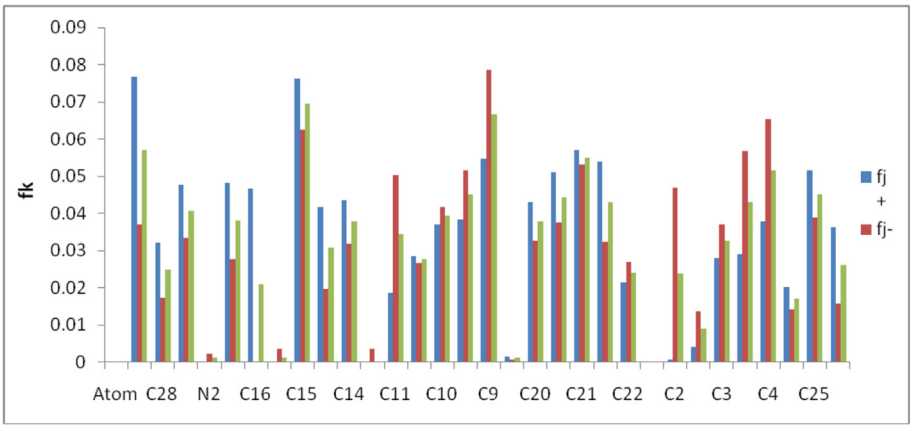

Fig. 5. Graphical view of Fukui function for 2(4-methoxyphenyl)-1,4,5-triphenyl-2,5-dihydro-1*H*-imidazole.

order for nucleophilic case is C28 > C15 > C21, the order of reactivity of electrophilic case is C9 > C4> C15 while the order of sites for free radical attack is C15 > C28 > C23 (Table 4 Suplementary Data).

3.9. Nonlinear optical properties

The static first order hyperpolarizability β (0,0,0) of the molecule was calculated.

The static first hyperpolarizability $\beta = (\beta_x^2+\beta_y^2+\beta_z^2)^{1/2}$

where

$\beta_x = \beta_{xxx}+\beta_{xyy}+\beta_{xzz}$

$\beta_y = \beta_{yyy}+\beta_{xxy}+\beta_{yzz}$

$\beta_z = \beta_{zzz}+\beta_{xxz}+\beta_{yyz}$

The calculated field independent first hyperpolarizability of the compound was 7.18×10^{-30} esu. Compared with the β value of urea 0.13×10^{-30} esu, the title compound was found to be a good candidate [42] as an NLO material due to its increased π conjugation length which enhanced the hyperpolarizability of the molecule.

4. Conclusions

2-(4-methoxyphenyl)-1,4,5-triphenyl-2,5-dihydro-1*H*-imidazole was synthesised, characterised by FT-IR, ^{1}H NMR and Single Crystal X-ray analysis. Single crystal analysis showed that the molecule belonged to monoclinic system and $P2_1/c$ space group. Each unit cell contained four molecules which were planar. Geometric parameters, vibrational, electronic spectra, Fukui indices, HOMO-LUMO of the title compound were studied on the basis of DFT calculations at B3LYP/6-31G basis set. Nucleophilic and electrophilic behaviour of specific sites in the molecule was analysed using Fukui function. Electronic spectra showed transition bands indicating that the molecule could be used as electron transport material. Results showed that the title compound could be used as a good NLO active material also. Proper designing, synthesis and theoretical investigation of this kind of compounds can lead to the development of suitable electron transport materials for organic electronic devices.

Appendix A. Supplementary data

Supplementary crystallographic data for this article is available in Cambridge Crystallographic information (CCDC 1910169). It can be obtained free of charge via http://www.ccdc.cam.ac.uk/.

Acknowledgement

The authors thank SAIF CUSAT, Cochin India for Single Crystal and ^{1}HNMR analysis.

References

[1] Y. Ozkay, I. Iskar, Z. Incesu, A. Ge, Eur. J. Med. Chem. 45 (2010) 3320–3328.
[2] F. Elahian, M. Akbari, M. Ghasemi, N. Behtoomee, M. Taheri, M. Amini, Lett. Drug Des. Discov. 11 (2014) 840–843.
[3] D. Sharma, B. Narasimhan, P. Kumar, V. Judge, R. Narang, E. Clercq, J. Balzarini, Eur. J. Med. Chem. 44 (2009) 2347–2353.
[4] (a) R. Thomas, M. Hossain, Y. Sheena Mary, K.S. Resmi, S. Armaković, S.J. Armaković, A.K. Nanda, V.K. Ranjan, G. Vijayakumar, C.V. Alsenoy, J. Mol. Struct. 1158 (173) (2018) 156–175;
(b) R.V. Shingalapur, K.M. Hosamani, R.S. Keri, Eur. J. Med. Chem. 44 (2009) 4244–4248.
[5] H. Stark, A. Hüls, X. Ligneau, K. Puranda, H. Pertza, J. Arrang, J. Schwartz, W. Schunacka, Arch. Pharm. 331 (1998) 211–218.
[6] H. Yanagisawa, Y. Amemiya, T. Kanazaki, Y. Shimoji, K. Fujimoto, Y. Kitahara, T. Sada, M. Mizuno, M. Ikeda, S. Miyamoto, Y. Furukawa, H. KoikeJ, Med. Chem. 39 (1996) 323–338.
[7] Y. Shen, J. Li, S. Chen, J. Wan, Y. Zhao, Z. Lu, M. Li, L. Yang, X. Yu, D. Chen, Z. Pan, Chemistry 2 (2017) 11206–11210.
[8] W. Li, L. Yao, H. Liu, Z. Wang, S. Zhang, R. Xiao, H. Zhang, P. Lu, B. Yang, J. Mater. Chem. 2 (2014) 4733–4736.
[9] J. Tagare, D.K. Dubey, J. HueiJou, S. Vaidyanathan, Dyes Pigments 160 (2019) 944–956.
[10] J. Tagare, S. Sudheendran, S. Prabha, D.K. Dubey, R. Ashokkumar Yadav, J. HueiJou, S. Vaidyanathan, Org. ele. 62 (2018) 419–428.
[11] S. Naka, H. Okada, H. Onnagawa, Appl. Phys. Lett. 76 (2000) 197–199.
[12] D.F. O'Brien, M.A. Baldo, M.E. Thompson, S.R. Forrest, Appl. Phys. Lett. 74 (1999) 442–444.
[13] N. Li, P. Wang, S.L. Lai, W. Liu, C.S. Lee, S.T. Lee, Z. Liu, Adv. Mater. 22 (2010) 527–530.
[14] A.P. Kulkarni, C.J. Tonzola, A. Babel, S.A. Jenekhe, Chem. Mater. 16 (23) (2004) 4556–4573.
[15] B. Wang, G. Mu, J. Tan, Z. Lei, J. Jin, L. Wang, J. Mater. Chem. C 3 (2015) 7709–7719.
[16] T. Shan, Z. Gao, X. Tang, X. He, Y. Gao, J. Li, X. Sun, Y. Liu, H. Liu, B. Yang, P. Lu, Y. Ma, Dyes Pigments 142 (2017) 189–197.
[17] X. Qiu, J. Shi, X. Xu, Y. Lu, Q. Sun, S. Xue, W. Yang, Dyes Pigments 147 (2017) 6–15.
[18] W.C. Chen, Y. Yuan, Y. Xiong, L. Andrey, A.L. Rogach, Q.X. Tong, C.S. Lee, Appl. Mater. Interfaces 9 (2017) 26268–26278.
[19] V. Thanikachalam, E. Sarojpurani, J. Jayabharathi, P. Jeeva, New J. Chem. 41 (2017) 2443–2457.
[20] S.S. Reddy, W. Cho, V.G. Sree, S.H. Jin, Dyes Pigments 134 (2016) 315–324.
[21] D. Tavgeniene, G. Krucaite, U. Baranauskyte, J.Z. Wu, H.Y. Su, C.W. Huang, C.H. Chang, S. Grigalevicius, Dyes Pigments 137 (2017) 615–621.

[22] M.J. Frisch, G.W. Trucks, H.B. Schlegel, G.E. Scuseria, M.A. Robb, J.R. Cheeseman, G. Scalmani, V. Barone, B. Mennucci, G.A. Petersson, H. Nakatsuji, M. Caricato, X. Li, H.P. Hratchian, A.F. Izmaylov, J. Bloino, G. Zheng, J.L. Sonnenberg, M. Hada, M. Ehara, K. Toyota, R. Fukuda, J. Hasegawa, M. Ishida, T. Nakajima, Y. Honda, O. Kitao, H. Nakai, T. Vreven, J.A. Montgomery Jr., J.E. Peralta, F. Ogliaro, M. Bearpark, J.J. Heyd, E. Brothers, K.N. Kudin, V.N. Staroverov, T. Keith, R. Kobayashi, J. Normand, K. Raghavachari, A. Rendell, J.C. Burant, S.S. Iyengar, J. Tomasi, M. Cossi, N. Rega, J.M. Millam, M. Klene, J.E. Knox, J.B. Cross, V. Bakken, C. Adamo, J. Jaramillo, R. Gomperts, R.E. Stratmann, O. Yazyev, A.J. Austin, R. Cammi, C. Pomelli, J.W. Ochterski, R.L. Martin, K. Morokuma, V.G. Zakrzewski, G.A. Voth, P. Salvador, J.J. Dannenberg, S. Dapprich, A.D. Daniels, O. Farkas, J.B. Foresman, J.V. Ortiz, J. Cioslowski, D.J. Fox, Gaussian 09, Revision B.01, Gaussian, Inc., Wallingford CT, 2010.
[23] C. Peng, P.Y. Ayala, H.B. Schlegel, M.J. Frisch, J.Comp Chem. 17 (1996) 49–56.
[24] R. Dennington, T. Keith, J. Millam, GaussView, Version 5, Semichem Inc., Shawnee Mission KS, 2009.
[25] (a) J.P. Perdew, K. Burke, M. Ernzerhof, Phys. Rev. Lett. 77 (1996) 3865–3868; (b) C. Adamo, V. Barone, J. Chem. Phys. 110 (1999) 6158–6170.
[26] J. Autschbach, T. Ziegler, S.J.A. Van Gisbergen, E.J. Baerends, J. Chem. Phys. 116 (2002) 6930–6940.
[27] G. Velmurugan, B.K. Ramamoorthi, P. Venuvanalingam, Phys. Chem. Chem. Phys. 39 (2014) 21157–21171.
[28] V. Kannan, K. Sreekumar, J Mol.catal.A Chem. 376 (2013) 34–39.
[29] S. Ray, A. Das, J.Molstruc. 1089 (2015) 146–152.
[30] H.G. Silver, J.L. Wood, Trans. Faraday Soc. 60 (1964) 5–9.
[31] R. Ramasamy, J. Appl. Spectrosc. 80 (2013) 492–498.
[32] R. Ramasamy, Arm.J.Phys. 8 (2015) 51–55.
[33] R.A. Marcus, Mod. Phys. 65 (1993) 599–610.
[34] R.G. Parr, Horizons of Quantum Chemistry, Springer, 1980, pp. 5–15.
[35] O. Tamer, N. Dege, D. Avcı, Y. Atalay, I.O. Ilhan, M. Çadır, Spectrochim. Acta Part A Mol. Biomol. Spectrosc. 137 (2015) 1387–1396.
[36] J. Zevallos, A. Toro-Labbe, J. Chil. Chem. Soc. 48 (2003) 39–47.
[37] V. Balachandran, M. Murugan, V. Karpagam, M. Karnan, G. Ilango, Spectrochim. Acta, Part A 130 (2014) 367–375.
[38] K. Fukui, Science 218 (1982) 747–754.
[39] R.G. Parr, W. Yang, J. Am. Chem. Soc. 106 (1984) 4049–4050.
[40] P.K. Chattaraj, B. Maiti, U. Sarkar, J. Phys. Chem. A 107 (2003) 4973–4975.
[41] C. Morell, A. Grand, A. Toro-Labbe, J. Phys. Chem. A 109 (2005) 205–212.
[42] M. Adant, M. Dupuis, J.L. Bredas, Int. J. Quantum Chem. 56 (1995) 497–507.